FERMILAB-PUB-07-553-E

Search for Randall-Sundrum gravitons with 1 fb^{-1} of data from $p\overline{p}$ collisions at $\sqrt{s} = 1.96$ TeV

V.M. Abazov[36], B. Abbott[76], M. Abolins[66], B.S. Acharya[29], M. Adams[52], T. Adams[50], E. Aguilo[6], S.H. Ahn[31], M. Ahsan[60], G.D. Alexeev[36], G. Alkhazov[40], A. Alton[65,a], G. Alverson[64], G.A. Alves[2], M. Anastasoaie[35], L.S. Ancu[35], T. Andeen[54], S. Anderson[46], B. Andrieu[17], M.S. Anzelc[54], Y. Arnoud[14], M. Arov[61], M. Arthaud[18], A. Askew[50], B. Åsman[41], A.C.S. Assis Jesus[3], O. Atramentov[50], C. Autermann[21], C. Avila[8], C. Ay[24], F. Badaud[13], A. Baden[62], L. Bagby[53], B. Baldin[51], D.V. Bandurin[60], S. Banerjee[29], P. Banerjee[29], E. Barberis[64], A.-F. Barfuss[15], P. Bargassa[81], P. Baringer[59], J. Barreto[2], J.F. Bartlett[51], U. Bassler[18], D. Bauer[44], S. Beale[6], A. Bean[59], M. Begalli[3], M. Begel[72], C. Belanger-Champagne[41], L. Bellantoni[51], A. Bellavance[51], J.A. Benitez[66], S.B. Beri[27], G. Bernardi[17], R. Bernhard[23], I. Bertram[43], M. Besançon[18], R. Beuselinck[44], V.A. Bezzubov[39], P.C. Bhat[51], V. Bhatnagar[27], C. Biscarat[20], G. Blazey[53], F. Blekman[44], S. Blessing[50], D. Bloch[19], K. Bloom[68], A. Boehnlein[51], D. Boline[63], T.A. Bolton[60], G. Borissov[43], T. Bose[78], A. Brandt[79], R. Brock[66], G. Brooijmans[71], A. Bross[51], D. Brown[82], N.J. Buchanan[50], D. Buchholz[54], M. Buehler[82], V. Buescher[22], S. Bunichev[38], S. Burdin[43,b], S. Burke[46], T.H. Burnett[83], C.P. Buszello[44], J.M. Butler[63], P. Calfayan[25], S. Calvet[16], J. Cammin[72], W. Carvalho[3], B.C.K. Casey[51], N.M. Cason[56], H. Castilla-Valdez[33], S. Chakrabarti[18], D. Chakraborty[53], K.M. Chan[56], K. Chan[6], A. Chandra[49], F. Charles[19,‡], E. Cheu[46], F. Chevallier[14], D.K. Cho[63], S. Choi[32], B. Choudhary[28], L. Christofek[78], T. Christoudias[44,†], S. Cihangir[51], D. Claes[68], Y. Coadou[6], M. Cooke[81], W.E. Cooper[51], M. Corcoran[81], F. Couderc[18], M.-C. Cousinou[15], S. Crépé-Renaudin[14], D. Cutts[78], M. Ćwiok[30], H. da Motta[2], A. Das[46], G. Davies[44], K. De[79], S.J. de Jong[35], E. De La Cruz-Burelo[65], C. De Oliveira Martins[3], J.D. Degenhardt[65], F. Déliot[18], M. Demarteau[51], R. Demina[72], D. Denisov[51], S.P. Denisov[39], S. Desai[51], H.T. Diehl[51], M. Diesburg[51], A. Dominguez[68], H. Dong[73], L.V. Dudko[38], L. Duflot[16], S.R. Dugad[29], D. Duggan[50], A. Duperrin[15], J. Dyer[66], A. Dyshkant[53], M. Eads[68], D. Edmunds[66], J. Ellison[49], V.D. Elvira[51], Y. Enari[78], S. Eno[62], P. Ermolov[38], H. Evans[55], A. Evdokimov[74], V.N. Evdokimov[39], A.V. Ferapontov[60], T. Ferbel[72], F. Fiedler[24], F. Filthaut[35], W. Fisher[51], H.E. Fisk[51], M. Ford[45], M. Fortner[53], H. Fox[23], S. Fu[51], S. Fuess[51], T. Gadfort[83], C.F. Galea[35], E. Gallas[51], E. Galyaev[56], C. Garcia[72], A. Garcia-Bellido[83], V. Gavrilov[37], P. Gay[13], W. Geist[19], D. Gelé[19], C.E. Gerber[52], Y. Gershtein[50], D. Gillberg[6], G. Ginther[72], N. Gollub[41], B. Gómez[8], A. Goussiou[56], P.D. Grannis[73], H. Greenlee[51], Z.D. Greenwood[61], E.M. Gregores[4], G. Grenier[20], Ph. Gris[13], J.-F. Grivaz[16], A. Grohsjean[25], S. Grünendahl[51], M.W. Grünewald[30], J. Guo[73], F. Guo[73], P. Gutierrez[76], G. Gutierrez[51], A. Haas[71], N.J. Hadley[62], P. Haefner[25], S. Hagopian[50], J. Haley[69], I. Hall[66], R.E. Hall[48], L. Han[7], K. Hanagaki[51], P. Hansson[41], K. Harder[45], A. Harel[72], R. Harrington[64], J.M. Hauptman[58], R. Hauser[66], J. Hays[44], T. Hebbeker[21], D. Hedin[53], J.G. Hegeman[34], J.M. Heinmiller[52], A.P. Heinson[49], U. Heintz[63], C. Hensel[59], K. Herner[73], G. Hesketh[64], M.D. Hildreth[56], R. Hirosky[82], J.D. Hobbs[73], B. Hoeneisen[12], H. Hoeth[26], M. Hohlfeld[22], S.J. Hong[31], S. Hossain[76], P. Houben[34], Y. Hu[73], Z. Hubacek[10], V. Hynek[9], I. Iashvili[70], R. Illingworth[51], A.S. Ito[51], S. Jabeen[63], M. Jaffré[16], S. Jain[76], K. Jakobs[23], C. Jarvis[62], R. Jesik[44], K. Johns[46], C. Johnson[71], M. Johnson[51], A. Jonckheere[51], P. Jonsson[44], A. Juste[51], D. Käfer[21], E. Kajfasz[15], A.M. Kalinin[36], J.R. Kalk[66], J.M. Kalk[61], S. Kappler[21], D. Karmanov[38], P. Kasper[51], I. Katsanos[71], D. Kau[50], R. Kaur[27], V. Kaushik[79], R. Kehoe[80], S. Kermiche[15], N. Khalatyan[51], A. Khanov[77], A. Kharchilava[70], Y.M. Kharzheev[36], D. Khatidze[71], H. Kim[32], T.J. Kim[31], M.H. Kirby[54], M. Kirsch[21], B. Klima[51], J.M. Kohli[27], J.-P. Konrath[23], M. Kopal[76], V.M. Korablev[39], A.V. Kozelov[39], D. Krop[55], T. Kuhl[24], A. Kumar[70], S. Kunori[62], A. Kupco[11], T. Kurča[20], J. Kvita[9], F. Lacroix[13], D. Lam[56], S. Lammers[71], G. Landsberg[78], P. Lebrun[20], W.M. Lee[51], A. Leflat[38], F. Lehner[42], J. Lellouch[17], J. Leveque[46], P. Lewis[44], J. Li[79], Q.Z. Li[51], L. Li[49], S.M. Lietti[5], J.G.R. Lima[53], D. Lincoln[51], J. Linnemann[66], V.V. Lipaev[39], R. Lipton[51], Y. Liu[7,†], Z. Liu[6], L. Lobo[44], A. Lobodenko[40], M. Lokajicek[11], P. Love[43], H.J. Lubatti[83], A.L. Lyon[51], A.K.A. Maciel[2], D. Mackin[81], R.J. Madaras[47], P. Mättig[26], C. Magass[21], A. Magerkurth[65], P.K. Mal[56], H.B. Malbouisson[3], S. Malik[68], V.L. Malyshev[36], H.S. Mao[51], Y. Maravin[60], B. Martin[14], R. McCarthy[73], A. Melnitchouk[67], A. Mendes[15], L. Mendoza[8], P.G. Mercadante[5], M. Merkin[38], K.W. Merritt[51], J. Meyer[22,d], A. Meyer[21], T. Millet[20], J. Mitrevski[71], J. Molina[3], R.K. Mommsen[45], N.K. Mondal[29], R.W. Moore[6], T. Moulik[59], G.S. Muanza[20], M. Mulders[51], M. Mulhearn[71], O. Mundal[22], L. Mundim[3], E. Nagy[15], M. Naimuddin[51], M. Narain[78], N.A. Naumann[35], H.A. Neal[65], J.P. Negret[8], P. Neustroev[40], H. Nilsen[23], H. Nogima[3], A. Nomerotski[51], S.F. Novaes[5], T. Nunnemann[25], V. O'Dell[51], D.C. O'Neil[6], G. Obrant[40], C. Ochando[16], D. Onoprienko[60], N. Oshima[51], J. Osta[56], R. Otec[10], G.J. Otero y Garzón[51], M. Owen[45], P. Padley[81], M. Pangilinan[78], N. Parashar[57], S.-J. Park[72], S.K. Park[31], J. Parsons[71], R. Partridge[78], N. Parua[55], A. Patwa[74], G. Pawloski[81], B. Penning[23],

M. Perfilov[38], K. Peters[45], Y. Peters[26], P. Pétroff[16], M. Petteni[44], R. Piegaia[1], J. Piper[66], M.-A. Pleier[22], P.L.M. Podesta-Lerma[33,c], V.M. Podstavkov[51], Y. Pogorelov[56], M.-E. Pol[2], P. Polozov[37], B.G. Pope[66], A.V. Popov[39], C. Potter[6], W.L. Prado da Silva[3], H.B. Prosper[50], S. Protopopescu[74], J. Qian[65], A. Quadt[22,d], B. Quinn[67], A. Rakitine[43], M.S. Rangel[2], K. Ranjan[28], P.N. Ratoff[43], P. Renkel[80], S. Reucroft[64], P. Rich[45], M. Rijssenbeek[73], I. Ripp-Baudot[19], F. Rizatdinova[77], S. Robinson[44], R.F. Rodrigues[3], M. Rominsky[76], C. Royon[18], P. Rubinov[51], R. Ruchti[56], G. Safronov[37], G. Sajot[14], A. Sánchez-Hernández[33], M.P. Sanders[17], A. Santoro[3], G. Savage[51], L. Sawyer[61], T. Scanlon[44], D. Schaile[25], R.D. Schamberger[73], Y. Scheglov[40], H. Schellman[54], P. Schieferdecker[25], T. Schliephake[26], C. Schwanenberger[45], A. Schwartzman[69], R. Schwienhorst[66], J. Sekaric[50], H. Severini[76], E. Shabalina[52], M. Shamim[60], V. Shary[18], A.A. Shchukin[39], R.K. Shivpuri[28], V. Siccardi[19], V. Simak[10], V. Sirotenko[51], P. Skubic[76], P. Slattery[72], D. Smirnov[56], J. Snow[75], G.R. Snow[68], S. Snyder[74], S. Söldner-Rembold[45], L. Sonnenschein[17], A. Sopczak[43], M. Sosebee[79], K. Soustruznik[9], M. Souza[2], B. Spurlock[79], J. Stark[14], J. Steele[61], V. Stolin[37], D.A. Stoyanova[39], J. Strandberg[65], S. Strandberg[41], M.A. Strang[70], M. Strauss[76], E. Strauss[73], R. Ströhmer[25], D. Strom[54], L. Stutte[51], S. Sumowidagdo[50], P. Svoisky[56], A. Sznajder[3], M. Talby[15], P. Tamburello[46], A. Tanasijczuk[1], W. Taylor[6], J. Temple[46], B. Tiller[25], F. Tissandier[13], M. Titov[18], V.V. Tokmenin[36], T. Toole[62], I. Torchiani[23], T. Trefzger[24], D. Tsybychev[73], B. Tuchming[18], C. Tully[69], P.M. Tuts[71], R. Unalan[66], S. Uvarov[40], L. Uvarov[40], S. Uzunyan[53], B. Vachon[6], P.J. van den Berg[34], R. Van Kooten[55], W.M. van Leeuwen[34], N. Varelas[52], E.W. Varnes[46], I.A. Vasilyev[39], M. Vaupel[26], P. Verdier[20], L.S. Vertogradov[36], M. Verzocchi[51], F. Villeneuve-Seguier[44], P. Vint[44], P. Vokac[10], E. Von Toerne[60], M. Voutilainen[68,e], R. Wagner[69], H.D. Wahl[50], L. Wang[62], M.H.L.S Wang[51], J. Warchol[56], G. Watts[83], M. Wayne[56], M. Weber[51], G. Weber[24], A. Wenger[23,f], N. Wermes[22], M. Wetstein[62], A. White[79], D. Wicke[26], G.W. Wilson[59], S.J. Wimpenny[49], M. Wobisch[61], D.R. Wood[64], T.R. Wyatt[45], Y. Xie[78], S. Yacoob[54], R. Yamada[51], M. Yan[62], T. Yasuda[51], Y.A. Yatsunenko[36], K. Yip[74], H.D. Yoo[78], S.W. Youn[54], J. Yu[79], A. Zatserklyaniy[53], C. Zeitnitz[26], T. Zhao[83], B. Zhou[65], J. Zhu[73], M. Zielinski[72], D. Zieminska[55], A. Zieminski[55], L. Zivkovic[71], V. Zutshi[53], and E.G. Zverev[38]

(The DØ Collaboration)

[1]*Universidad de Buenos Aires, Buenos Aires, Argentina*
[2]*LAFEX, Centro Brasileiro de Pesquisas Físicas, Rio de Janeiro, Brazil*
[3]*Universidade do Estado do Rio de Janeiro, Rio de Janeiro, Brazil*
[4]*Universidade Federal do ABC, Santo André, Brazil*
[5]*Instituto de Física Teórica, Universidade Estadual Paulista, São Paulo, Brazil*
[6]*University of Alberta, Edmonton, Alberta, Canada, Simon Fraser University, Burnaby, British Columbia, Canada, York University, Toronto, Ontario, Canada, and McGill University, Montreal, Quebec, Canada*
[7]*University of Science and Technology of China, Hefei, People's Republic of China*
[8]*Universidad de los Andes, Bogotá, Colombia*
[9]*Center for Particle Physics, Charles University, Prague, Czech Republic*
[10]*Czech Technical University, Prague, Czech Republic*
[11]*Center for Particle Physics, Institute of Physics, Academy of Sciences of the Czech Republic, Prague, Czech Republic*
[12]*Universidad San Francisco de Quito, Quito, Ecuador*
[13]*Laboratoire de Physique Corpusculaire, IN2P3-CNRS, Université Blaise Pascal, Clermont-Ferrand, France*
[14]*Laboratoire de Physique Subatomique et de Cosmologie, IN2P3-CNRS, Universite de Grenoble 1, Grenoble, France*
[15]*CPPM, IN2P3-CNRS, Université de la Méditerranée, Marseille, France*
[16]*Laboratoire de l'Accélérateur Linéaire, IN2P3-CNRS et Université Paris-Sud, Orsay, France*
[17]*LPNHE, IN2P3-CNRS, Universités Paris VI and VII, Paris, France*
[18]*DAPNIA/Service de Physique des Particules, CEA, Saclay, France*
[19]*IPHC, Université Louis Pasteur et Université de Haute Alsace, CNRS, IN2P3, Strasbourg, France*
[20]*IPNL, Université Lyon 1, CNRS/IN2P3, Villeurbanne, France and Université de Lyon, Lyon, France*
[21]*III. Physikalisches Institut A, RWTH Aachen, Aachen, Germany*
[22]*Physikalisches Institut, Universität Bonn, Bonn, Germany*
[23]*Physikalisches Institut, Universität Freiburg, Freiburg, Germany*
[24]*Institut für Physik, Universität Mainz, Mainz, Germany*
[25]*Ludwig-Maximilians-Universität München, München, Germany*
[26]*Fachbereich Physik, University of Wuppertal, Wuppertal, Germany*
[27]*Panjab University, Chandigarh, India*
[28]*Delhi University, Delhi, India*

[29] Tata Institute of Fundamental Research, Mumbai, India
[30] University College Dublin, Dublin, Ireland
[31] Korea Detector Laboratory, Korea University, Seoul, Korea
[32] SungKyunKwan University, Suwon, Korea
[33] CINVESTAV, Mexico City, Mexico
[34] FOM-Institute NIKHEF and University of Amsterdam/NIKHEF, Amsterdam, The Netherlands
[35] Radboud University Nijmegen/NIKHEF, Nijmegen, The Netherlands
[36] Joint Institute for Nuclear Research, Dubna, Russia
[37] Institute for Theoretical and Experimental Physics, Moscow, Russia
[38] Moscow State University, Moscow, Russia
[39] Institute for High Energy Physics, Protvino, Russia
[40] Petersburg Nuclear Physics Institute, St. Petersburg, Russia
[41] Lund University, Lund, Sweden, Royal Institute of Technology and Stockholm University, Stockholm, Sweden, and Uppsala University, Uppsala, Sweden
[42] Physik Institut der Universität Zürich, Zürich, Switzerland
[43] Lancaster University, Lancaster, United Kingdom
[44] Imperial College, London, United Kingdom
[45] University of Manchester, Manchester, United Kingdom
[46] University of Arizona, Tucson, Arizona 85721, USA
[47] Lawrence Berkeley National Laboratory and University of California, Berkeley, California 94720, USA
[48] California State University, Fresno, California 93740, USA
[49] University of California, Riverside, California 92521, USA
[50] Florida State University, Tallahassee, Florida 32306, USA
[51] Fermi National Accelerator Laboratory, Batavia, Illinois 60510, USA
[52] University of Illinois at Chicago, Chicago, Illinois 60607, USA
[53] Northern Illinois University, DeKalb, Illinois 60115, USA
[54] Northwestern University, Evanston, Illinois 60208, USA
[55] Indiana University, Bloomington, Indiana 47405, USA
[56] University of Notre Dame, Notre Dame, Indiana 46556, USA
[57] Purdue University Calumet, Hammond, Indiana 46323, USA
[58] Iowa State University, Ames, Iowa 50011, USA
[59] University of Kansas, Lawrence, Kansas 66045, USA
[60] Kansas State University, Manhattan, Kansas 66506, USA
[61] Louisiana Tech University, Ruston, Louisiana 71272, USA
[62] University of Maryland, College Park, Maryland 20742, USA
[63] Boston University, Boston, Massachusetts 02215, USA
[64] Northeastern University, Boston, Massachusetts 02115, USA
[65] University of Michigan, Ann Arbor, Michigan 48109, USA
[66] Michigan State University, East Lansing, Michigan 48824, USA
[67] University of Mississippi, University, Mississippi 38677, USA
[68] University of Nebraska, Lincoln, Nebraska 68588, USA
[69] Princeton University, Princeton, New Jersey 08544, USA
[70] State University of New York, Buffalo, New York 14260, USA
[71] Columbia University, New York, New York 10027, USA
[72] University of Rochester, Rochester, New York 14627, USA
[73] State University of New York, Stony Brook, New York 11794, USA
[74] Brookhaven National Laboratory, Upton, New York 11973, USA
[75] Langston University, Langston, Oklahoma 73050, USA
[76] University of Oklahoma, Norman, Oklahoma 73019, USA
[77] Oklahoma State University, Stillwater, Oklahoma 74078, USA
[78] Brown University, Providence, Rhode Island 02912, USA
[79] University of Texas, Arlington, Texas 76019, USA
[80] Southern Methodist University, Dallas, Texas 75275, USA
[81] Rice University, Houston, Texas 77005, USA
[82] University of Virginia, Charlottesville, Virginia 22901, USA and
[83] University of Washington, Seattle, Washington 98195, USA

(Dated: October 17, 2007)

Using 1 fb^{-1} of data from $p\overline{p}$ collisions at $\sqrt{s} = 1.96$ TeV at the Fermilab Tevatron collider collected by the D0 detector, we search for decays of Kaluza-Klein excitations of the graviton in the Randall-Sundrum model of extra dimensions to e^+e^- and $\gamma\gamma$. We set 95% confidence level upper limits on the production cross section times branching fraction which translate into lower limits on the mass of the lightest excitation between 300 and 900 GeV for values of the coupling $k/\overline{M}_{Pl}$ between 0.01 and 0.1.

PACS numbers: 13.85.Rm, 04.50.+h, 12.60.-i

The large difference between the Planck scale, $M_{Pl} \approx 10^{16}$ TeV, and the weak scale presents a strong indication that the standard model is incomplete. In the presence of this hierarchy of scales it is not possible to stabilize the Higgs boson mass at the low values required by experimental data without an excessive amount of fine-tuning unless there is some, as yet unknown, physics at the TeV scale.

Randall and Sundrum have suggested a model [1] in which the fundamental scale of gravity is near the weak scale and gravity appears so feeble because it is exponentially suppressed by the existence of a fifth dimension and a warped space-time metric. Standard model fields would be confined to one 3-brane (a 4-dimensional subspace of this 5-dimensional space) and gravity originates at another 3-brane. Only gravitons propagate in the bulk between these two branes. The apparent weakness of gravity originates from the small overlap of the graviton wave function with the standard model fields in the fifth dimension.

This model predicts a tower of Kaluza-Klein excitations as the 4-dimensional manifestation of the graviton propagating in 5-dimensional space. In the following we refer to these as RS (Randall-Sundrum) gravitons. The massless zero-mode couples with gravitational strength. The massive modes couple with similar strength as the weak interaction. Their properties are quantified by two parameters, the mass of the first massive excitation M_1 and the dimensionless coupling constant to standard model fields, $k/\overline{M}_{Pl}$, where $\overline{M}_{Pl} = M_{Pl}/\sqrt{8\pi}$ is the reduced Planck scale. To address the hierarchy problem without the need for fine-tuning M_1 should be in the TeV range and $0.01 < k/\overline{M}_{Pl} < 0.1$ [2]. For these values the first massive RS graviton G is a narrow resonance with a width much smaller than the resolution of the D0 detector. If kinematically accessible, RS gravitons can be resonantly produced in high energy particle collisions. They decay into pairs of fermions or bosons.

In this Letter we consider decays into e^+e^- and $\gamma\gamma$ pairs. We search for these as resonances in the e^+e^- and $\gamma\gamma$ invariant mass spectrum from 1 fb^{-1} of data collected using the D0 detector at the Fermilab Tevatron collider between October 2002 and February 2006. In the Tevatron protons and antiprotons collide at $\sqrt{s} = 1.96$ TeV. D0 has previously published searches for RS gravitons [3] and excluded $M_1 < 250$ GeV for $k/\overline{M}_{Pl} = 0.01$ and $M_1 < 785$ GeV for $k/\overline{M}_{Pl} = 0.1$ at 95% confidence level with 260 pb^{-1} of data. CDF has recently submitted for publication searches that exclude $M_1 < 889$ GeV for $k/\overline{M}_{Pl} = 0.1$ [4] based on 1.3 fb^{-1} of data.

The D0 detector [5, 6] consists of tracking detectors, calorimeters, and a muon spectrometer. The tracker employs silicon microstrips close to the beam and concentric cylinders of scintillating fibers in a 2 T axial magnetic field. The liquid-argon/uranium sampling calorimeter has an electromagnetic section that is 20 radiation lengths deep, backed up by a hadronic section. The calorimeter is divided into a central section covering $|\eta| \leq 1.1$ and two endcap calorimeters extending coverage to $|\eta| \leq 4.2$. The luminosity is monitored by two arrays of plastic scintillation counters located on the inside faces of the endcap calorimeters. The pseudorapidity $\eta = -\ln[\tan(\theta/2)]$ and θ is the polar angle with respect to the proton beam direction. The azimuthal angle is denoted by ϕ and we measure object separation in the detector in terms of $\Delta R = \sqrt{(\Delta\phi)^2 + (\Delta\eta)^2}$. We denote the momentum component transverse to the beam direction with p_T. Readout is controlled by a three-level trigger system.

Since both electrons and photons result in electromagnetic showers with very similar signatures in our detector, we can define an inclusive selection that provides good efficiency for selecting e^+e^- and $\gamma\gamma$ final states. In particular we require clusters of energy depositions in the electromagnetic calorimeter that are consistent with the expected shower profile using a χ^2 test and have less than 3% of their energy leaking into the hadronic calorimeter section. We require that the cluster is well isolated with less than 7% of the cluster energy in an annular isolation cone with $0.2 < \Delta R < 0.4$ around the cluster centroid and less than 2 GeV for the sum of the p_T of all tracks with $0.05 < \Delta R < 0.4$ with respect to the cluster centroid. To accept both electrons and photons we do not require a matched track. We start with a data set of 34 million events triggered on one or two electromagnetic showers with p_T thresholds between 15 and 35 GeV. We select events in which there are at least two such clusters with $p_T > 25$ GeV in the central calorimeter with $|\eta| < 1.1$. Including clusters in the end calorimeters would add little acceptance for decay products of massive objects. In the collider data we find 43639 events that satisfy these selection criteria with the invariant mass of the two clusters $M_{ee/\gamma\gamma} > 60$ GeV.

Within the standard model, the Drell-Yan process and diphoton production give rise to e^+e^- and $\gamma\gamma$ final states. The invariant mass spectrum for these is expected to fall towards higher masses except for the $Z \rightarrow e^+e^-$ resonance. We model these backgrounds using a Monte Carlo simulation with the PYTHIA [7] event generator using the CTEQ6L parton distribution functions [8], followed by a GEANT-based [9] detector simulation. Another source of events is the misidentification of one or two jets as electron or photon candidates. The shape of the invariant mass spectrum of this source of events is estimated from data by selecting events with energy clusters in the electromagnetic calorimeter that are not consistent with electromagnetic showers and fail the χ^2 test for the shower profile. The absence of the Z resonance in the background spectrum in Fig. 1 confirms that this sample has no significant contamination from e^+e^- final states.

We fit the shape of the invariant mass spectrum from the data near the Z resonance ($60 < M_{ee/\gamma\gamma} < 140$ GeV) with a superposition of the spectrum from Monte Carlo predictions for the standard model processes and the spectrum expected from misidentified clusters. In the fit, the spectra from e^+e^- and $\gamma\gamma$ final states are normalized relative to each other by the leading order cross section from PYTHIA, the total number of events is fixed to the number of events observed in the data, and the fraction f of all events that have misidentified clusters is the only free parameter. We obtain best agreement with the data for $f = 0.21 \pm 0.01$. The spectra are shown in Figure 1. Trigger thresholds affect the shapes near the low mass end of the fit window. We account for this by assigning a systematic uncertainty on the value of f. At masses above 100 GeV the trigger is fully efficient.

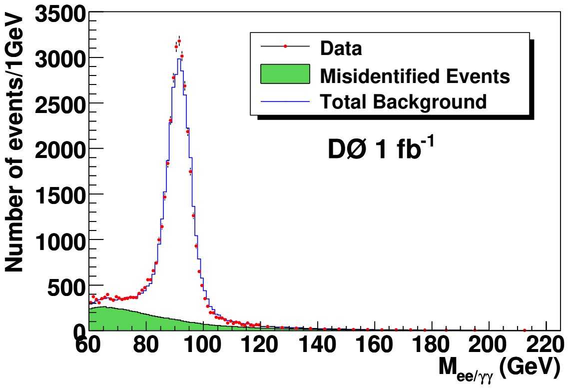

FIG. 1: Invariant mass spectrum from data (points). Superimposed is the fitted total background shape from standard model processes including events with misidentified clusters (open histogram) and the fitted contribution from events with misidentified clusters alone (shaded histogram).

We compare the invariant mass spectrum of our background model with the fitted value of f to the data at higher masses. As shown in Figure 2, we find agreement between background model and data in the high-mass range. There is a slight mismatch in the mass resolution at the Z peak between our Monte Carlo simulation and the data. We verified that this does not affect the predictions of the background model at higher masses.

From the fitted number of $p\overline{p} \to e^+e^- + X$ events (most of them in the Z resonance), the acceptance and efficiency from the Monte Carlo simulation, and the calculated standard model cross section, we determine the integrated luminosity of the data sample. All Monte-Carlo derived efficiencies are multiplied by 0.96 so that the efficiency from the $Z \to e^+e^-$ Monte Carlo simulation agrees with the efficiencies measured in $Z \to e^+e^-$ data. The leading order cross section for the e^+e^- final state with $60 < M_{ee} < 130$ GeV from PYTHIA is 178 pb. We multiply this by a next-to-leading order (NLO) K-factor of 1.34 [10]. This gives 985 ± 35 pb^{-1}. The uncertainty in this number is dominated by the uncertainty in the cross section from parton distribution functions. We do not include uncertainties on efficiencies and acceptances because these cancel in the limit calculation. This value is in agreement with the number determined using the luminosity counters (1036 ± 63 pb^{-1}) [11].

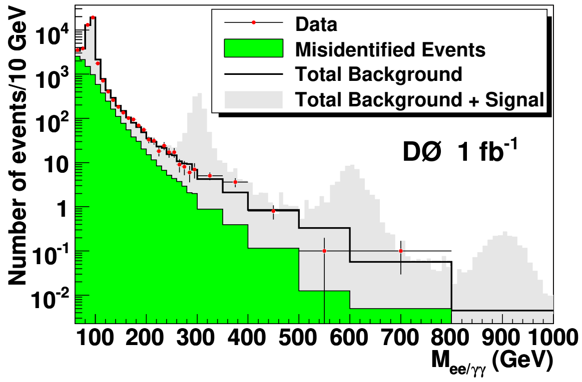

FIG. 2: Invariant mass spectrum from data (points). Superimposed is the fitted total background shape from standard model processes including events with misidentified clusters (open histogram) and the fitted contribution from events with misidentified clusters alone (shaded histogram). The grey shaded histogram shows the signal expected from gravitons with $M_1 = 300$, 600, and 900 GeV and $k/\overline{M}_{Pl} = 0.1$ on top of the total background.

We determine the signal acceptance and efficiency using a Monte Carlo simulation of RS gravitons with $200 < M_1 < 1000$ GeV using PYTHIA and GEANT. Systematic uncertainties in the signal efficiency originate from detector resolution (1-11%), parton distribution functions (0.2-5.5%), electron and photon identification efficiencies (1.4%), and the finite signal Monte Carlo sample size (0.5%). Contributions to the uncertainty in the background prediction are from the finite size of Monte Carlo and data samples (2-24%), parton distribution functions (2-10%), the mass dependence of the NLO K-factor (5%), and the uncertainty in the trigger thresholds (1%). In some cases the uncertainties vary with the invariant mass value.

We compute upper limits for the production cross section of RS gravitons times branching fraction into e^+e^- final states at 95% confidence level by comparing the observed and expected numbers of events in a sliding mass window. The width of the window was optimized for maximum sensitivity using the Monte Carlo simulation and varies from 20 GeV for $M_1 = 200$ GeV to 120 GeV for $M_1 = 950$ GeV. We use a Bayesian approach to integrate over all important input parameters such as signal efficiency, background prediction, and integrated luminosity, using a Gaussian prior with width equal to the estimated uncertainties in the parameters [12]. For the RS graviton production cross section we use a flat prior. To compute the limits, we use the integrated luminosity determined from the Z signal, which gives us a more pre-

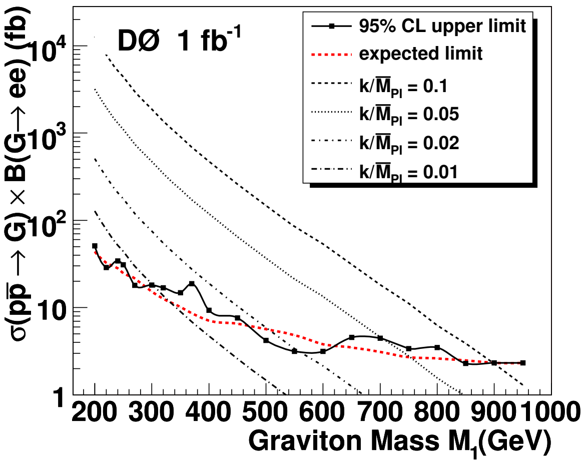

FIG. 3: 95% confidence level upper limit on $\sigma(p\overline{p} \to G + X) \times B(G \to e^+e^-)$ from 1 fb^{-1} of data compared with the expected limit and the theoretical predictions for different couplings $k/\overline{M}_{Pl}$.

cise normalization than the direct luminosity measurement. Figure 3 shows the limits as a function of invariant mass compared to predictions from the Randall-Sundrum model and Table I tabulates the results. Based on the observed and expected numbers of events we obtain limits on $\sigma(p\overline{p} \to G + X) \times B(G \to e^+e^-/\gamma\gamma)$. We divide by $B(G \to e^+e^-/\gamma\gamma)/B(G \to e^+e^-) = 3$ [13] to convert these to the quoted limits on $\sigma(p\overline{p} \to G + X) \times B(G \to e^+e^-)$.

Using the cross section predictions from the Randall-Sundrum model with the same K-factor as for the standard model processes [15], we set upper limits on the coupling $k/\overline{M}_{Pl}$ as a function of M_1. This is shown in Figure 4 and tabulated in Table I. For $k/\overline{M}_{Pl} = 0.01(0.1)$ we can exclude masses below 300(900) GeV at 95% confidence level.

In summary, we have searched for RS gravitons as resonances in the e^+e^- and $\gamma\gamma$ invariant mass spectrum from about 1 fb^{-1} of data from the Fermilab Tevatron collider. We find good agreement of the observed spectrum with standard model predictions and set lower limits on the mass of the first massive RS graviton at 95% confidence level of 300 GeV for $k/\overline{M}_{Pl} = 0.01$ and of 900 GeV for $k/\overline{M}_{Pl} = 0.1$. These are the tightest direct limits on RS gravitons to date.

We thank the staffs at Fermilab and collaborating institutions, and acknowledge support from the DOE and NSF (USA); CEA and CNRS/IN2P3 (France); FASI, Rosatom and RFBR (Russia); CAPES, CNPq, FAPERJ, FAPESP and FUNDUNESP (Brazil); DAE and DST (India); Colciencias (Colombia); CONACyT (Mexico); KRF and KOSEF (Korea); CONICET and UBACyT (Argentina); FOM (The Netherlands); Science and Technology Facilities Council (United Kingdom); MSMT and GACR (Czech Republic); CRC Program, CFI, NSERC and WestGrid Project (Canada); BMBF and DFG (Germany); SFI (Ireland); The Swedish Research Council (Sweden); CAS and CNSF (China); Alexander von Humboldt Foundation; and the Marie Curie Program.

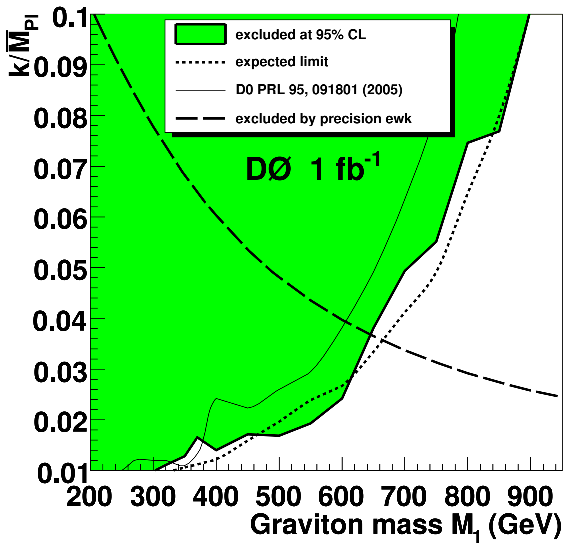

FIG. 4: 95% confidence level upper limit on $k/\overline{M}_{Pl}$ versus graviton mass M_1 from 1 fb^{-1} of data compared with the expected limit and the previously published exclusion contour [3]. The area below the dashed line is excluded by precision electroweak measurements (see [14]).

[a] Visitor from Augustana College, Sioux Falls, SD, USA.
[b] Visitor from The University of Liverpool, Liverpool, UK.
[c] Visitor from ICN-UNAM, Mexico City, Mexico.
[d] Visitor from II. Physikalisches Institut, Georg-August-University Göttingen, Germany.
[e] Visitor from Helsinki Institute of Physics, Helsinki, Finland.
[f] Visitor from Universität Zürich, Zürich, Switzerland.
[†] Fermilab International Fellow.
[‡] Deceased.

[1] L. Randall and R. Sundrum, Phys. Rev. Lett. **83**, 3370 (1999); ibid., **83**, 4690 (1999).
[2] H. Davoudiasl, J. L. Hewett and T. G. Rizzo, Phys. Rev. Lett. **84**, 2080 (1999).
[3] D0 Collaboration, V.M. Abazov *et al.*, Phys. Rev. Lett. **95**, 091801 (2005).
[4] CDF Collaboration, T. Aaltonen *et al.*, arXiv:0707.2294 [hep-ex] and arXiv:0707.2524v1 [hep-ex] submitted to Phys. Rev. Letters.
[5] D0 Collaboration, S. Abachi *et al.*, Nucl. Instrum. Meth-

TABLE I: Input data for limit calculation and 95% confidence level limits on cross section times branching fraction and coupling. Quoted are the total uncertainties that are used in the limit calculation.

					$\sigma(p\overline{p} \to G + X) \times B(G \to e^+e^-)$ (fb)			$k/\overline{M}_{Pl}$	
M_1 (GeV)	window (GeV)	data	back-ground	signal efficiency	theory	expected limit	observed limit	expected limit	observed limit
200	190-210	88	83.8±7.3	0.208±0.030	12730	48.8	56.9	0.0061	0.0066
220	210-230	49	52.3±4.7	0.214±0.033	7861	36.5	32.2	0.0068	0.0064
240	230-250	41	37.1±3.7	0.211±0.038	5181	32.4	39.7	0.0079	0.0087
250	240-260	34	30.1±3.1	0.215±0.038	4417	28.5	35.9	0.0080	0.0090
270	250-290	40	44.0±4.5	0.297±0.026	2988	23.5	19.6	0.0088	0.0081
300	280-320	29	26.9±3.0	0.310±0.029	1885	16.6	19.9	0.0094	0.0102
320	300-340	22	18.3±2.0	0.318±0.036	1371	13.9	18.6	0.0100	0.0116
350	330-370	15	11.4±1.2	0.311±0.034	902	11.2	16.3	0.0111	0.0134
370	350-390	16	8.7±1.0	0.316±0.039	688	9.5	21.0	0.0118	0.0175
400	380-420	7	5.8±0.7	0.319±0.042	473	7.9	10.4	0.0129	0.0148
450	420-480	6	4.8±0.6	0.366±0.021	259	6.7	8.2	0.0161	0.0178
500	450-550	3	5.3±1.0	0.419±0.014	147	6.1	4.5	0.0203	0.0175
550	500-600	1	3.3±0.9	0.434±0.015	84.9	5.0	3.4	0.0243	0.0200
600	550-650	1	1.84±0.22	0.454±0.017	53.6	3.9	3.4	0.0271	0.0251
650	600-700	2	1.04±0.13	0.437±0.013	31.3	3.6	4.9	0.0340	0.0396
700	620-780	2	0.84±0.10	0.458±0.013	18.3	3.2	4.8	0.0419	0.0513
750	660-840	1	0.51±0.06	0.473±0.015	11.2	2.8	3.6	0.0500	0.0573
800	700-900	1	0.32±0.04	0.474±0.015	6.2	2.7	3.7	0.0659	0.0775
850	750-950	0	0.18±0.02	0.481±0.013	3.9	2.5	2.4	0.0814	0.0799
900	790-1010	0	0.11±0.02	0.475±0.014	2.3	2.4	2.5	0.1030	0.1051
950	840-1060	0	0.06±0.01	0.474±0.012	1.3	2.4	2.5	0.1366	0.1394

ods Phys. Res. A **338**, 185 (1994).

[6] D0 Collaboration, V.M. Abazov *et al.*, Nucl. Instrum. Methods Phys. Res. A **565**, 463 (2006).

[7] T. Sjöstrand *et al.*, Computer Physics Commun. **135**, 238 (2001).

[8] J. Pumplin *et al.*, JHEP **0207** 012 (2002); D. Stump *et al.*, JHEP **0310** 046 (2003).

[9] R. Brun and F. Carminati, CERN Program Library Long Writeup W5013 (1993).

[10] R. Hamberg, W. L. van Neerven and T. Matsuura, Nucl. Phys. B **359**, 343 (1991) [Erratum-ibid. B **644**, 403 (2002)].

[11] T.Andeen *et al.*, "The D0 experiment's integrated luminosity for Tevatron Run IIa", FERMILAB-TM-2365 (2007).

[12] I. Bertram *et al.*, "A recipe for the construction of confidence limits," FERMILAB-TM 2104 (2000).

[13] T. Han, J. D. Lykken, R.-J. Zhang, Phys. Rev. D **59**, 105006 (1999).

[14] H. Davoudiasl, J. L. Hewett, and T. G. Rizzo, Phys. Rev. D **63**, 075004 (2001).

[15] P. Mathews, V. Ravindran, K. Sridhar, and W. L. van Neerven, Nucl. Phys. B **713**, 333 (2005).